Heritability of individualized cortical network topography

Kevin M. Anderson[a,1], Tian Ge[b,c,d], Ru Kong[e,f,g,h], Lauren M. Patrick[a], R. Nathan Spreng[i,j], Mert R. Sabuncu[k,l,m], B. T. Thomas Yeo[e,f,g,m,n], and Avram J. Holmes[a,d,o]

[a]Department of Psychology, Yale University, New Haven, CT 06520; [b]Psychiatric and Neurodevelopmental Genetics Unit, Center for Genomic Medicine, Massachusetts General Hospital, Boston, MA 02114; [c]Stanley Center for Psychiatric Research, Broad Institute of Massachusetts Institute of Technology and Harvard, Cambridge, MA 02142; [d]Department of Psychiatry, Massachusetts General Hospital, Harvard Medical School, Boston, MA 02114; [e]Department of Electrical and Computer Engineering, Centre for Sleep and Cognition, National University of Singapore, Singapore 119077; [f]Department of Electrical and Computer Engineering, Centre for Translational Magnetic Resonance Research, National University of Singapore, Singapore 119077; [g]N.1 Institute for Health, National University of Singapore, Singapore 119077; [h]Institute for Digital Medicine, National University of Singapore, Singapore 119077; [i]Department of Neurology and Neurosurgery, Montreal Neurological Institute, McGill University, Montreal, QC H3A 0G4, Canada; [j]McConnell Brain Imaging Centre, McGill University, Montreal, QC H3A 0G4, Canada; [k]School of Electrical and Computer Engineering, Cornell University, Ithaca, NY 14850; [l]Meinig School of Biomedical Engineering, Cornell University, Ithaca, NY 14850; [m]Martinos Center for Biomedical Imaging, Massachusetts General Hospital, Charlestown, MA 02129; [n]National University of Singapore Graduate School for Integrative Sciences and Engineering, National University of Singapore, Singapore 119077; and [o]Department of Psychiatry, Yale University, New Haven, CT 06520

Human cortex is patterned by a complex and interdigitated web of large-scale functional networks. Recent methodological breakthroughs reveal variation in the size, shape, and spatial topography of cortical networks across individuals. While spatial network organization emerges across development, is stable over time, and is predictive of behavior, it is not yet clear to what extent genetic factors underlie interindividual differences in network topography. Here, leveraging a nonlinear multidimensional estimation of heritability, we provide evidence that individual variability in the size and topographic organization of cortical networks are under genetic control. Using twin and family data from the Human Connectome Project ($n = 1,023$), we find increased variability and reduced heritability in the size of heteromodal association networks (h^2: M = 0.34, SD = 0.070), relative to unimodal sensory/motor cortex (h^2: M = 0.40, SD = 0.097). We then demonstrate that the spatial layout of cortical networks is influenced by genetics, using our multidimensional estimation of heritability (h^2-multi; M = 0.14, SD = 0.015). However, topographic heritability did not differ between heteromodal and unimodal networks. Genetic factors had a regionally variable influence on brain organization, such that the heritability of network topography was greatest in prefrontal, precuneus, and posterior parietal cortex. Taken together, these data are consistent with relaxed genetic control of association cortices relative to primary sensory/motor regions and have implications for understanding population-level variability in brain functioning, guiding both individualized prediction and the interpretation of analyses that integrate genetics and neuroimaging.

heritability | individualized parcellation | resting-state | function brain networks | functional connectome

The cerebral cortex is organized into a tightly interdigitated set of large-scale functional networks. Seminal tract-tracing work in nonhuman primates first revealed the structural properties underlying the distributed and parallel organization of cortical networks (1). Subsequent resting-state functional connectivity MRI (fcMRI) analyses leveraged correlation patterns of intrinsic functional MRI (fMRI) signal fluctuations in humans (2) to establish a canonical network architecture that is broadly shared across the population (3–8). Yet, many individual-specific properties of brain network organization are lost when central tendencies are examined across large groups. The use of population-average network topographies has accelerated psychological and neuroscientific discovery, however there is growing recognition that the human brain is characterized by striking functional variability across individuals (9–15). As individualized approaches become increasingly popular for the study of human behavior and psychopathology (13,

16–18), there is growing need to quantify the heritable bases of population-level variability in functional network size and topography. Despite the fact that individual differences result from the convergence of both genetic and environmental influences, the extent to which the size and spatial patterning of cortical networks may reflect heritable features of brain function has not yet been systematically investigated.

Population-based neuroimaging studies have revealed core principles that govern the evolution (19), development (20), and organization (7, 8) of large-scale brain networks. In particular, fcMRI has been widely utilized to generate group-average network templates through the joint analyses of data across vast numbers of individuals. The topography of these population-based network solutions are closely coupled to cognitive function, and there is strong correspondence between the spatial structure of intrinsic (fcMRI) and extrinsic (task-evoked) networks of the human brain (21–23). Consistent with these observations, functional connectivity patterns track behavioral variability in the

Significance

The widespread use of population-average cortical parcellations has provided important insights into broad properties of human brain organization. However, the size, location, and spatial arrangement of regions comprising functional brain networks can vary substantially across individuals. Here, we demonstrate considerable heritability in both the size and spatial organization of individual-specific network topography across cortex. Genetic factors had a regionally variable influence on brain organization, such that heritability in network size, but not topography, was greater in unimodal relative to heteromodal cortices. These data suggest individual-specific network parcellations may provide an avenue to understand the genetic basis of variation in human cognition and behavior.

general population (24–26) and symptom expression in patients with psychiatric illness (27). Mounting evidence documents the heritable basis of large-scale brain network function (28–31) as well as the ability of functional brain connectivity to serve as a trait-like fingerprint that can distinguish individuals from a larger group (32, 33). The advent of neuroimaging genetic and brain gene expression data further permits study of the genetic, molecular, and cellular correlates of human brain function (34–36). Critically, however, the use of population-based network templates can obscure individual-specific features of brain organization (9), as there is substantial evidence for interindividual variability in the size, location, and topography of regions comprising distributed functional networks across the cortical sheet.

The presence of individual differences in connectome organization presents a challenge for neuroscientists studying the functional architecture of the human brain. The identification of genetic and developmental cascades that underpin population-level variability in brain function is partly dependent on whether a group network atlas aligns to the particular functional topography of an individual. As one example, reports of population-level variability in connectivity strengths across participant groups may in fact emerge from the misalignment of underlying functional networks, obscuring the distinction between individual differences in network connectivity and topography (37, 38). Moreover, personalized network parcellations may be preferable for predictive modeling, graph theoretic, and imaging genetic approaches in which the definition of an areal "unit" of cortex can influence downstream interpretations (39). While the size and shape of individualized networks are stable across time (40), predictive of behavior (13, 41), and refined over the course of development (42), the molecular and genetic bases of this variability in network size, location, and spatial arrangement remain to be established. Recent studies have shown that individual differences in functional connectivity are heterogeneous across the cortex, with greater variability in association cortex relative to unimodal regions (13, 15, 40, 43). This distribution may have practical implications for the heritability of network topographies in association cortices, pointing to potential relationships linking the spatial distribution of interindividual variation in functional connectivity, brain evolution, and development. Quantifying the heritability of individual-specific network topographies across the cortical sheet could provide new insights into the biological underpinnings of individual differences in human brain functions.

Although prior twin studies establish the heritability of functional connectivity strength within population-average network templates (28, 29, 31, 44, 45), the role of genetics in sculpting the spatial topography of the functional connectome has yet to be quantified. To directly address this open question, we couple a multisession hierarchical Bayesian model (MS-HBM) for estimating individual-specific cortical networks (13) with a nonlinear multidimensional estimation of heritability. This approach allows us to establish the extent to which genetic and environmental factors influence individual differences in network size and topography across the cortical sheet. In doing so, we provide evidence that interindividual variability in both the spatial extent and topographic organization of cortical networks are under genetic control.

Results

Interindividual Variability in Network Size Is Nonuniform across Heteromodal and Unimodal Cortices. We first characterized interindividual variability in the size of functional networks across the cortical sheet. Individual-specific network topographies for each Human Connectome Project (HCP) participant (46) were obtained from the method of Kong and colleagues (13), derived using a MS-HBM. For every participant, each vertex on the cortical surface was assigned to one of 17 canonical functional networks (8), based on both intraindividual and interindividual patterns of cortical resting-state correlation (Fig. 1A). Networks were broadly divided into those encompassing unimodal sensory and motor regions (i.e., Visual A/B/C, Somato/motor A/B, and Auditory), and those linked to heteromodal association cortex (i.e., Default A/B/C, Control A/B/C, Ventral Attention A/B, Dorsal Attention A/B, and Language). HCP cortical parcellations were identical to those of Kong and colleagues (13), who first detailed the MS-HBM approach and demonstrated that individualized network topographies are predictive of behavior. Parcellations were derived from surface-projected resting-state fMRI (rs-fMRI) data aligned to a surface-mesh group template (fs_LR32k). After masking of the midline, each participant was left with a 59,412-vertex array of network labels, where each vertex is assigned to one of 17 networks.

The spatial extent of each network within an individual was estimated as the summed surface area of all network labeled vertices, derived using each individual's FreeSurfer-estimated vertex surface area. The size of individualized cortical networks displayed nonuniform patterns of variability across individuals, as displayed in Fig. 1B. Between-participants variability in network size was quantified using coefficient of variation (see *Methods*), which corrects for baseline differences in average network surface area. Overall, areal size was significantly more variable among heteromodal networks relative to unimodal ($F(1,32) = 2.51$, $P = 0.017$; $M_{het} = 24.6$, SD = 5.3; $M_{uni} = 20.5$, SD = 2.4), an effect that remained if we used SD as a measure of variability rather than coefficient of variation ($F(1,32) = 2.6$, $P = 0.014$; $M_{het} = 5,236$, SD = 1,856; $M_{uni} = 4,800$, SD = 2,180). These data are in line with prior reports that interindividual variability in the strength of functional connectivity is greatest in heteromodal cortex (43), corresponding to territories with highest evolutionary cortical expansion and density of long-range functional connections (47, 48).

Reduced Heritability of Network Size in Heteromodal Relative to Unimodal Cortex. Interindividual differences in network connectivity strengths are partly attributable to genetic variation (29). However, the majority of the literature on the genetic bases of network architecture relies on population-level motifs derived by averaging data across large groups of spatially normalized individuals (28, 30, 45). To advance understanding of the biological bases of network organization, it is important to move from group-level parcellations to a level of granularity that is only accessible when studying network organization within the individual. Given that both the size and shape of individualized functional networks are tied to behavior (13, 17, 40, 42), it is critical to determine heritable sources of variation that govern the amount of cortex occupied by a given functional network.

Analyses revealed that the size of individualized networks were significantly heritable across all canonical large-scale functional territories (Fig. 2A). Heritabilities (h^2) were calculated using individualized network size (controlling for total surface area) and ranged between 0.23 to 0.60 (M = 0.36, SD = 0.09; Dataset S1A). Heritability of surface area for each network was estimated using sequential oligogenic linkage analysis routines [SOLAR (49)] and covaried for age, age^2, age × sex, age^2 × sex, total surface area, and FreeSurfer-derived estimated total intracranial volume. Suggesting broad consistency in the influence of genetic factors on the size of cortical networks across hemispheres, a significant positive correlation between left- and right-hemisphere heritability estimates was evident across the 17 networks (Fig. 2B; Pearson's r(15) = 0.61, $P = 0.0086$; Spearman's $r_s = 0.63$, $P = 0.009$). Notably, heritability was significantly greater within unimodal networks (h^2: M = 0.40, SD = 0.097) than networks within heteromodal (h^2: M = 0.34, SD = 0.070) association cortices (Fig. 2C; $F(1,32) = 2.36$, $P = 0.025$).

The above analyses covary for total surface area to account for global differences in cortical size; however, estimates of regional area can scale in a nonlinear fashion with total area (19). An additional set of analyses was conducted to account for such
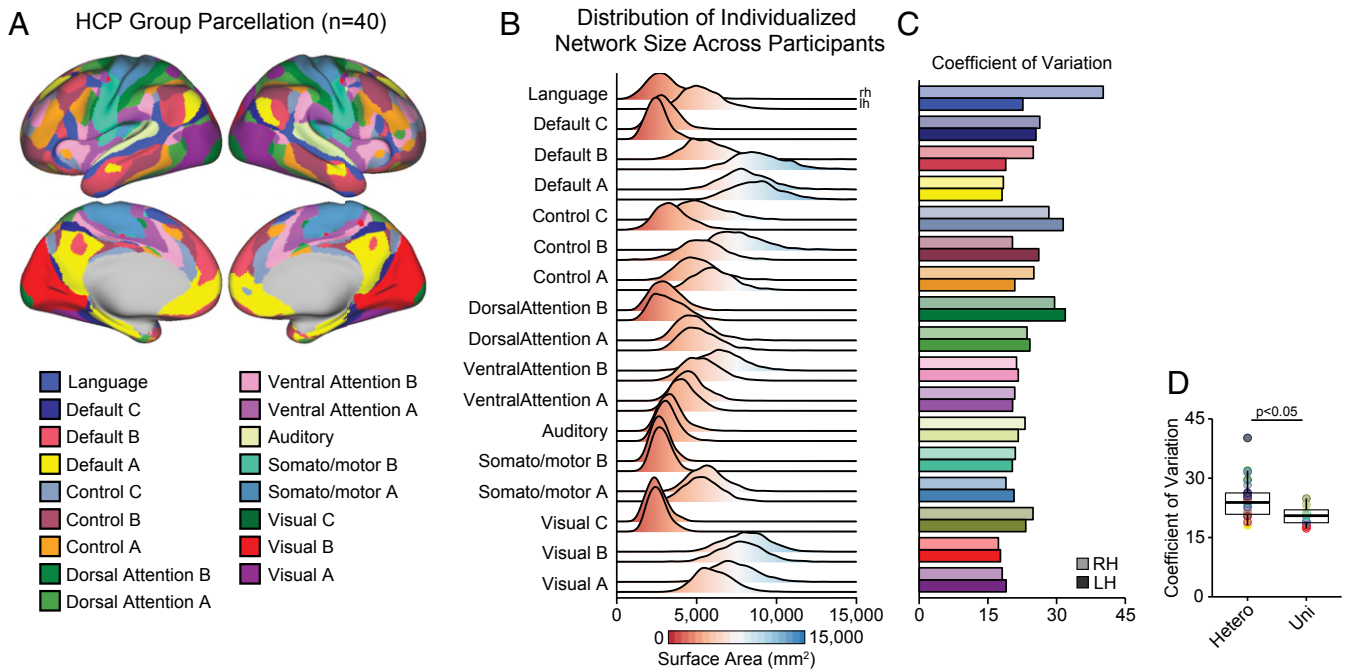
www.manaraa.com

Fig. 1. Individualized network size is more variable in heteromodal relative to unimodal cortex. (*A*) Individualized parcellations are composed of 17 canonical functional networks present in all HCP individuals, as defined by Kong and colleagues (13). (*B*) The ridge plot shows distributions of network size across all individuals, measured in mm^2 and separated by hemisphere (top ridge = right hemisphere, bottom ridge = left hemisphere). (*C*) Variability of individualized network size across all participants, measured with coefficient of variation, which corrects for differences in the total average size of each network. (*D*) Network sizes are significantly more variable within heteromodal (M = 24.6, SD = 5.3) relative to unimodal cortices (M = 20.5, SD = 2.4; $F(1,32) = 2.51$, $P = 0.017$). Hetero, heteromodal cortex; Uni, unimodal cortex.

allometric scaling of cortex. General additive modeling was used to conduct a log–log regression, relating the log of individualized network size to the log of total surface area, covarying for age and sex (*Methods*). In this context, a coefficient greater than 1 reflects positive areal scaling (greater network size relative to total surface area) and a coefficient less than 1 reflects negative scaling. We found that heteromodal networks had significantly greater positive scaling coefficients compared with unimodal networks (*SI Appendix*, Fig. S2*A*; $F(1,32) = 3.04$, $P = 0.0048$; $M_{het} = 1.09$, SD = 0.18; $M_{uni} = 0.92$, SD = 0.08). The heritability of allometrically adjusted network size was then estimated, revealing a pattern that was highly consistent to the results displayed in Fig. 2*A*. Specifically, the parcel-to-parcel correlation of linear versus allometrically adjusted h^2 was Spearman's $r_s = 0.95$, $P < 2.2 \times 10^{-16}$. We note that the finding of increased heritability of unimodal cortex versus heteromodal cortex did not attain statistical significance after allometric surface area adjustment (*SI Appendix*, Fig. S2*C*; $F(1,32) = 1.88$, $P = 0.069$).

Overall, these data demonstrate the substantial influence of genetic factors on the spatial extent of cortical networks across individuals. The results are consistent with the hypothesis that late-developing aspects of heteromodal association cortex are under relaxed genetic control relative to unimodal cortex (50). We emphasize that heritability reflects the degree that genetics explains individual differences in a trait within a given environmental context, not the degree to which a trait is evolutionary constrained or genetically encoded.

Heritability of Individualized Network Topography across Cortex. The connectivity strength of functional networks varies across individuals (32, 43). Individualized parcellation approaches have established similar patterns of interindividual variation in terms of cortical network topography, operationalized as the spatial configuration of a given network on the cortical sheet (11, 13).

Factors that may play a role in differentiating functional topography across individuals include mechanical tension of neuronal projections (51), cellular and molecular properties of cortex (52), variations in early cortical arealization by embryonic molecular patterning centers (53), and the fundamental role sensory input plays in shaping functional organization across the cortical sheet (54). However, the extent that variability in the spatial organization of cortical networks is genetically driven within the general population remains unknown.

Here, we establish that genetic factors influence individualized network topographies using a multidimensional estimator of heritability. In traditional heritability analyses, the variability of a continuous (e.g., height) or categorical (e.g., diagnosis) phenotype is decomposed into the relative effects of additive genetics (A), shared environment (C), and unique environment [E; ACE model (55)]. Network topography, however, is inherently multidimensional, since any given cortical vertex is categorically assigned to one of a set of functional networks. To account for this property of network organization, we developed an approach to estimate heritability from a linear or nonlinear phenotypic similarity matrix defined across individuals. Interindividual covariance of network shape was quantified using the Dice coefficient, which reflects the amount of spatial overlap for any given network and participant pair (see Fig. 3*D* for example). That is, higher Dice coefficients correspond to more similar network configurations. The observed Dice coefficients were variable across individuals as well as nonuniformly distributed across networks (Fig. 3*A*). The topographies of unimodal networks were overall more similar across individuals (Dice: M = 0.77, SD = 0.05) relative to heteromodal association networks (Dice: M = 0.55, SD = 0.06; $F(1,32) = 112.4$, $P = 5.35 \times 10^{-12}$). The increased topographic variability of association networks is consistent with prior reports of greater interindividual variation in accompanying patterns of long-range connectivity (43).
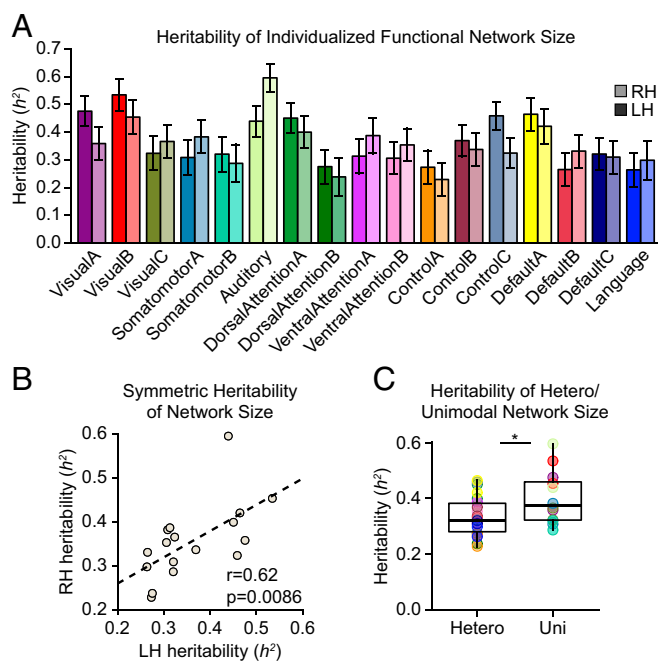
Fig. 2. Heritability of individualized network size is greater in unimodal relative to heteromodal networks. (*A*) Heritability of individual network size (controlling for total surface area) was estimated across 17 canonical functional networks using SOLAR (49), separately for each hemisphere. Error bars reflect 95% CIs. (*B*) The amount of variance explained by genetics (h^2) for each network was consistent across hemispheres, as revealed by a correlation of left- and right-hemisphere h^2 values ($r = 0.62$, $P = 0.0086$). Each dot in the correlation plot is a functional network. (*C*) Heritability of normalized individual network size was higher among unimodal/sensory networks relative to heteromodal association networks ($P = 0.025$). Each dot represents one of 17 cortical networks, split by hemisphere ($n = 34$). Hetero, heteromodal cortex; Uni, unimodal cortex.

Analysis of multidimensional heritability, denoted "h^2-multi," demonstrated that interindividual differences in network topography were significantly influenced by inherited genetics (Fig. 3*B*; h^2-multi: min = 0.12, max = 0.19, M = 0.14, SD = 0.015; Dataset S1*B*), after accounting for multiple testing corrections (Bonferroni false discovery rate correction, q's < 0.05). Fig. 3*C* displays the distribution of Dice coefficients reflecting interindividual similarity of network topography defined across all 17 cortical networks (i.e., "Overall" in Fig. 3*B*). Dice similarity was greater for monozygotic twins (left hemisphere [LH]: M = 0.70, SD = 0.026; right hemisphere [RH]: M = 0.69, SD = 0.024) and relative to dizygotic twins (LH: M = 0.66, SD = 0.028; RH: M = 0.65, SD = 0.028), siblings (LH: M = 0.66, SD = 0.026; RH: M = 0.65, SD = 0.028), and unrelated individuals (LH: M = 0.64, SD = 0.027; RH: M = 0.063, SD = 0.026), corresponding to a h^2-multi of 0.146 and 0.143 for left and right hemispheres, respectively. The degree of topographic heritability for each network was consistent across hemispheres (Spearman's rho = 0.68, $P = 0.0032$). Contrary to estimates of individualized network size, the heritability of network topographies did not differ between unimodal and heteromodal networks ($F(1,32) = 0.63$, $P = 0.54$). We emphasize that h^2-multi is calculated from a matrix of subject-to-subject pairwise similarities (i.e., Dice coefficients), reflecting the number of vertices with the same network label between any given pair of individuals. Because individual parcellations vary, the specific vertices that contribute to any particular Dice coefficient vary as well. Overall, these data advance a heritability estimation technique to demonstrate that the spatial organization of functional networks is influenced by genetic factors.

We next quantified local genetic control of network architecture across the cortical sheet. Our findings detailed above show that the heritability of network topography is uniform across cortex when averaging within individual networks (Fig. 3). Prior work, however, indicates significant spatial heterogeneity of heritable aspects of cortical anatomy (56–58). Here, we demonstrate that genetic influences on local network topography are also spatially variable across cortex, with the greatest heritability observed within the precuneus as well as dorsal aspects of parietal, prefrontal, and posterior parietal cortices (Fig. 4*A*). Multidimensional heritability estimates were calculated in the same manner as above, whereby a Dice coefficient matrix represented the participant-to-participant similarity of network topography. In this analysis, however, we only consider individualized network labels falling within a given region of interest (ROI; radius = 10 vertices) at each point on the cortical sheet. Fig. 4*B* illustrates example participant pairs with high and low Dice coefficients for an ROI in the precuneus. Critically, some participant pairs possess almost entirely nonoverlapping network assignments within a given patch of cortex (Fig. 4*B*), highlighting the need for individualized parcellations to study of neurobiological variability across the population. Of note, we did not observe a clear dissociation between unimodal and heteromodal cortices in terms of local network heritability. That is, heritability estimates did not differ between regions canonically associated with sensorimotor networks (M = 0.150, SD = 0.037) relative to association networks (M = 0.145, SD = 0.037; $F(1,32) = 1.59$, $P = 0.12$; Dataset S1 *C and D*). Together, these results indicate the heritable basis of network organization is variable across cortex and support further research into the biological determinants of network topography.

Discussion

The use of population-average network templates has provided foundational insights into the macroscopic functional organization of the human brain. However, individual-specific features of brain network architecture are obscured when collapsing data across large groups of participants. Methodological advances make it possible to measure individualized features of functional networks in vivo, promising to yield biological insight into the genetic, molecular, and cellular bases of cortical brain organization. Here, leveraging a form of multidimensional heritability analysis, we demonstrate that a substantial portion of the population-level variability in the size and spatial arrangement of cortical networks is under the influence of genetic factors. In HCP data ($n = 1,023$), the size (i.e., cortical surface area) of individualized networks showed considerable interindividual variation, which was most pronounced in higher-order heteromodal relative to unimodal sensorimotor networks (Fig. 1). We demonstrated that individualized network size was heritable for all 17 examined cortical networks but was most pronounced within unimodal, relative to heteromodal cortices (Fig. 2). Next, we established the heritability of individualized network spatial organization, or topography, for all cortical functional networks (Fig. 3). Although topographic heritability was broadly consistent between cortical networks, we observed substantial spatial heterogeneity in the influence of genetic factors across the cortical sheet (Fig. 4). Together, this work advances an analytic framework for measuring heritability of multidimensional traits to establish the extent that individual-specific features of functional network organization are influenced by inherited genetics.

The estimation of the heritability of multidimensional traits, such as the brain's functional network architecture, is challenging given that traditional approaches are designed for continuous (e.g., height) or binary (e.g., diagnosis) phenotypes (59). In the present study, we describe a method for estimating heritability from any matrix of participant-wise similarity metrics. Dice coefficients were used to quantify between-participants similarity of
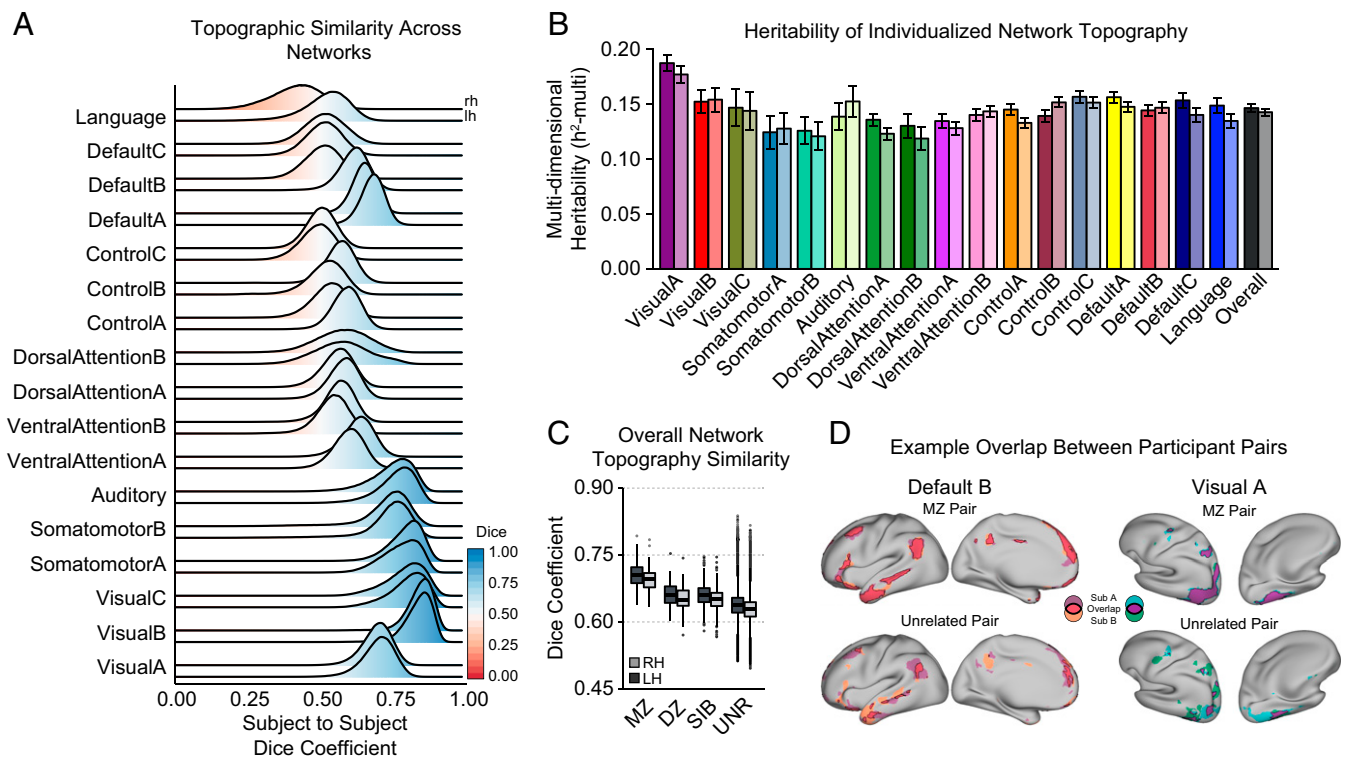
Fig. 3. Individualized network topography is heritable across all networks. (*A*) The ridge plot displays distributions of interindividual Dice coefficients across each network. Higher Dice coefficients reflect higher spatial overlap of a network for a given pair of individuals. Topography of unimodal networks were overall more similar across individuals, relative to heteromodal cortex. (*B*) Significant heritability was observed across all examined 17 cortical networks (q < 0.01; range = 0.12 to 0.19, mean = 0.14), which was symmetric across hemispheres (r_s = 0.68, P = 0.0032). (*C*) Boxplots show higher Dice similarity of overall network organization between MZ pairs, relative to DZ, sibling, and unrelated participant pairings. (*D*) Individual examples illustrate HCP participants with a high and low dice overlap for Default B (high = 0.78; low = 0.29) and Visual C (high = 0.93; low = 0.59) networks. SIB, sibling; UNR, unrelated.

network topography, but this approach is generalizable to other commonly studied neuroscientific phenotypes, such as patterns of anatomical similarity (60) or morphometricity (61). We have made the associated code freely available to the community (https://github.com/kevmanderson/h2_multi), along with analytic pipelines for all analyses. This work provides the basis for further elaboration of multidimensional heritability techniques, such as genetic correlation, that could reveal patterns of shared genetic variance with psychological phenotypes (13, 42). Individualized network parcellations also hold promise for understanding

psychiatric disorders (16), which are often heritable (62). Identifying shared genetic substrates between individualized features of network organization and psychiatric illness will be important as individualized approaches become increasingly adopted in clinical neuroscientific research.

Here, we demonstrated that a significant proportion of the variance in network size and topography is explained by genetics, which could emerge through many possible biological pathways. For instance, the individual differences in cortical arealization that influence network organization may be determined early in
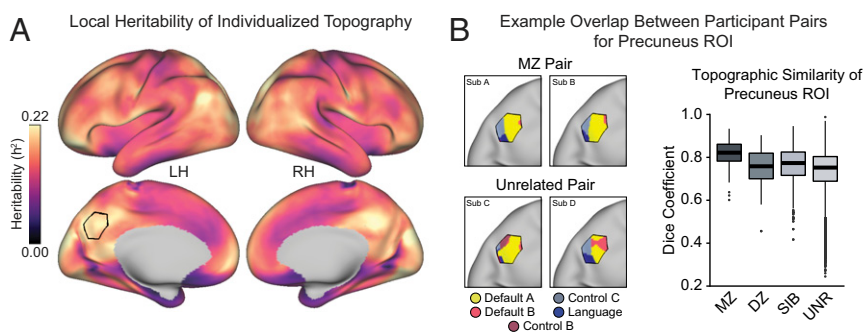

Fig. 4. Local heritability of individualized network topography. (*A*) Multidimensional heritability of network topography estimated for every vertex, using an ROI at each point on the cortical sheet (radius = 10 vertices). Individualized network labels in each ROI were used to compute a participant-to-participant Dice similarity matrix, reflecting the similarity of network assignments within a given cortical area. Warmer colors indicate higher heritability of network assignments, for instance reflecting greater similarity among twins and siblings than unrelated individuals. (*B*) Example participant pairs with high and low Dice overlap of network labels for an ROI in the precuneus. Dice similarity was higher between MZ twins, relative to DZ, sibling, and unrelated participant pairs. SIB, sibling; UNR, unrelated; LH, left hemisphere; RH, right hemisphere.

Anderson et al.
Heritability of individualized cortical network topography

neurodevelopment. That is, the cellular fate and areal identity of early cortical progenitor cells are specified in embryonic periods by spatial gradients of molecular transcription factors (63, 64), which may vary across individuals. The ability of genetic variation to shape these early developmental processes is supported by a recent genome-wide association study (GWAS) documenting that common genetic polymorphisms linked to cortical surface area were enriched among regulatory elements of neural progenitor neural cells (65). The topography of cortical functional networks may also be influenced by cortical neuroanatomy, such as cortical morphology and patterns of structural connectivity. In this context, biomechanical processes such as axonal tension, intracranial pressure, and the differential growth of cortical layers are thought to influence cortical folding (51, 66), which may in turn constrain the topography of functional networks. Further, the size and shape of functional network boundaries may be sculpted by thalamocortical connections that refine patterns of cortical arealization across development (54). Experimentally modulating thalamic afferents can substantially impact cortical morphology and size in a pathway specific manner (67, 68). Critically, however, heritability analyses cannot disentangle the specific biological processes that influence cortical network size or topography. Rather, our data support the importance of future work utilizing statistical genetic approaches to identify the biological cascades that influence functional network topography across the cortical sheet (65).

The emergence of analytic frameworks for capturing individualized network architectures is both a technical and theoretical advance, providing the opportunity to link cognition and behavior to population-level variability in brain organization. Landmark research has shown that individuals can be identified by patterns of whole-brain functional connectivity, conceptualized as a functional "fingerprint" (25, 32). The analogy to a fingerprint is apt. For instance, broad classes of fingerprint types exhibit a high degree of heritability, despite ridge patterns of any fingerprint being entirely unique (69). Likewise, the brain is organized into a core functional network architecture that nevertheless exhibits distinctive features in a trait-like manner at the level of the individual (40). Here, we demonstrate that the distinguishing topographic features of the brain, including variability in network organization and size, are influenced by inherited genetic factors (Fig. 3). Such data provide a potential "upper bound" on the explainable variance because of additive genetic variation and highlight the utility of future research probing the genetic mechanisms underlying interindividual differences in functional network organization across the lifespan.

Consistent with prior work examining population-average network templates, the current study provides support for the genetic bases of core features of brain function (28–30, 45, 70–72). The degree of heritability for functional network size is in line with prior estimates demonstrating that ~40 to 60% of the variance in within-network connectivity is explained by genetics (28, 29). Of note, we emphasize that our data reflect a snapshot of heritability estimates for a given sample in early adulthood and that the influence of genetic factors may vary across developmental periods (73). Perhaps counterintuitively, phenotypic heritability generally increases from childhood through adulthood, possibly reflecting genotype–environment interactions as individuals engage in behaviors that reinforce genetically influenced traits (74). Although, there is evidence that the reverse is true in late adulthood, such that heritability decreases with age (75). Future work should also examine whether environmental factors such as early life stress or adversity may also impact cortical network topography and connectivity (76). Experience is also critical for the emergence of functional selectivity in some brain regions, such as the face-responsive inferotemporal cortex, which may in turn influence patterns of network connectivity and affiliation (77). Given recent evidence of the developmentally dynamic nature of functional

network organization (42), it will be important to utilize imaging genetic data, such as the Adolescent Brain Cognitive Development (ABCD) study (78), to quantify the age-dependent influence of genetic factors on cortical network formation.

Our twin and family-based analyses compliment GWAS studies identifying structural genetic polymorphisms linked to functional brain phenotypes, which are often defined according to template or group-level network atlases (31, 79). These results motivate further investigation into the genetic bases of individualized cortical network properties using imaging genetic data, such as the UK Biobank and ABCD study. The family-based heritability estimates described here are a first approximation of the upper bound of variance that can be accounted for by common genetic polymorphisms. However, additional GWAS studies are needed to identify specific genetic variants and biological processes that may influence cortical network topography.

Higher-order association networks are consistently more variable than unimodal sensorimotor networks in terms of both relative network size (Fig. 1C) and topographic network similarity (Fig. 3). These observations are consistent with evidence that heteromodal cortex has greater interindividual variance in functional connectivity (43). The increased variability of heteromodal network size coincided with lower estimates of heritability, relative to the individualized size of unimodal networks (Fig. 2C). These data are in line with theories that late-developing aspects of cortex are more sensitive to environmental influences and extrinsic sources of network sculpting (50). That is, higher-order networks are the most distal (or "untethered") from both early embryonic signaling gradients and thalamus-mediated sensory inputs (50). However, we did not observe heteromodal versus unimodal differences in heritability for measures of network topography (Figs. 3 and 4) as we did for individualized network size.

The present study should be interpreted in light of several limitations. First, our analyses assume that participants have been brought into a common anatomical space, but we cannot rule out the role of interindividual differences in alignment accuracy. Here, we used sophisticated surface-based alignment techniques from the HCP that rely on multimodal areal features of cortex rather than cortical folding patterns and anatomical landmarks (80). However, interindividual alignment is still subject to error. We also emphasize that heritability estimates of network topography are dependent upon the accuracy and assumptions of the parcellation approach. We also note that our heritability estimation, calculated from a linear or nonlinear phenotypic similarity matrix, is equivalent to the heritability of the intrinsic multidimensional trait that generates the participant-wise phenotypic similarity (59) (see Methods) and is therefore different from traditional heritability analysis of a scalar phenotype (e.g., height) unless the similarity matrix is spanned by a one-dimensional vector. Our analyses test whether the size of a cortical network is under heritable genetic influence. Spatial network topography differs from more commonly used measures of functional connectivity strength; however, the two metrics are not necessarily orthogonal. For instance, functional connectivity strength may vary as a function of topographic network size, or vice versa. Most individualized parcellation techniques are sensitive to functional connectivity strength in addition to spatial organization, and therefore future work is required to disentangle the interdependence of functional network size and connectivity strength (13, 41).

In conclusion, this paper advances a multidimensional heritability technique to establish the heritability of individualized cortical functional networks in terms of both network size and topography. We found that the size of heteromodal cortical networks was more variable and less heritable relative to unimodal networks, in line with the protracted developmental maturation of higher-order cortex that may allow for increased influence of the environment. Individualized network topography was similarly more variable among heteromodal networks, but heritability was approximately equivalent for all cortical functional networks.

www.manaraa.com

However, heritability analysis of local network architecture revealed a nonuniform influence of genetic factors on network organization across cortex. Together, these data establish that the size and topography of cortical functional networks are influenced by genetic factors, providing a foundation for future work disentangling the biological mechanisms that govern individual variances in brain organization.

Methods

HCP. The HCP is a large community-based sample of twins and nuclear family members, assessed on a comprehensive set of neuroimaging and behavioral batteries. HCP analyses initially comprised 1,029 participants that were successfully processed through the individualized network parcellation approach of Kong and colleagues (13) known as the MS-HBM. HCP twin zygosity was determined by genotyped data when possible ($n = 410$), otherwise self-report was used to identify pairs of monozygotic (MZ) and dizygotic (DZ) twins ($n = 76$). If imaging data were not available for one twin in a pair, the usable participant was designated a "singleton" for later heritability analyses. The final sample consisted of $n = 1,023$ individuals ($n_{MZ} = 274$; $n_{DZ} = 160$, $n_{nontwin} = 482$, $n_{singleton} = 107$). See Table 1 for basic demographics across groups.

Measuring Individualized Network Organization and Size. Individualized network parcellations were derived from HCP rs-fMRI surface data, aligned to the fs_LR32k group space using the Multimodal Surface Matching (MSM) All areal feature-based registration (81). Methodological details of the MS-HBM approach that produced the individualized parcellations have been previously published (13); however, we present key details here. Multiband rs-fMRI data collected on Siemens 3T Skyra scanners from the HCP S1200 release were analyzed. A key feature of the MS-HBM approach is that it incorporates both intraindividual and interindividual patterns of variability to define individualized network boundaries. HCP data are particularly suited for this method since rs-fMRI runs were collected across two separate sessions across 2 d, allowing for well-powered estimates of inter- and intraindividual variance. Individual resting-state runs were 15 min in length and were acquired at an isotropic resolution of 2 mm and TR of 0.72 s (82, 83). Surface-based preprocessing of rs-fMRI data began with minimally preprocessed HCP MSMAll FMRIB's independent component analysis (ICA)-based X-noiseifier (ICA-FIX) data on a group surface template [fs_LR32k (84)]. Additional preprocessing included nuisance regression, temporal censoring, and spatial smoothing.

A held-out training set of 40 HCP participants were used to derive the necessary group-level parcellation (Fig. 1A) and model parameters, such as interindividual variability, for the MS-HSM method. For each participant, each of the 59,412 bihemispheric vertices on the cortical sheet was assigned to one of the 17 canonical functional networks (8). Individualized parcellations were transformed from the fs_LR32k to the fsaverage6 group template using the HCP workbench. The surface area of each individualized cortical parcel was then estimated using FreeSurfers *mris_anatomical_stats* utility. The size of each cortical network for an individual was estimated as the summed surface area of all network vertices. Network size was calculated separately for each hemisphere and then divided by total hemispheric area to quantify proportional size of a network on the cortical sheet. All cortical surface figures were created using the HCP workbench (85).

Heritability of Individualized Network Size. The heritability of individualized network size was estimated using SOLAR (49), covarying for age, sex, age², age × sex, age² × sex, total surface area, and FreeSurfer-derived intracranial volume. Bonferroni correction of significance thresholds was used to account for 34 independent tests of heritability. Cross-hemisphere consistency (Fig. 2B) was tested by correlating left- and right-hemisphere heritability estimates across all 17 cortical networks.

Dice Similarity of Network Topography. Participant-to-participant similarity of individualized network topography was measured using the Dice–Sørensen formula, where the coefficient for a given network reflects the following:

$$\text{Dice Similarity} = \frac{2|X_i \cap Y_i|}{|X_i| + |Y_i|},$$

where X_i and Y_i are the network labels for network i for participants X and Y, $\cap$ represents the intersection between participant network labels, and $|\cdot|$ represents the total number of vertices in each set (i.e., cardinality).

Multidimensional Heritability Analysis. Consider an M-dimensional trait $Y = [y_1, \ldots, y_m] = [y_{im}]_{N \times M}$ and a multivariate variance component model: $Y = G + E$, where G and E are $N \times M$ matrices representing the additive genetic effects and unique environmental factors, respectively. Assume $\text{vec}(G) \sim N(0, \Sigma_G \otimes K)$, $\text{vec}(E) \sim N(0, \Sigma_E \otimes I)$, where $\text{vec}(\otimes)$ is the matrix vectorization operator that converts a matrix into a vector by stacking its columns, $\otimes$ is the Kronecker product of matrices, Σ_G is the genetic covariance matrix, and Σ_E is the environmental covariance matrix. The genetic and environmental covariance matrices can be estimated using a moment-matching method: $\hat{\Sigma}_G = \frac{1}{v_k} Y^\top (K - \tau I) Y$, $\hat{\Sigma}_E = \frac{1}{v_k} Y^\top (\kappa I - \tau K) Y$, where $\tau = \text{tr}(K)/N$, $\kappa = \text{tr}(K^2)/N$, $v_K = N(\kappa - \tau^2)$ (59). The single nucleotide polymorphism (SNP) heritability of a multidimensional trait Y is defined by $\hat{h}^2 = \frac{\text{tr}(\hat{\Sigma}_G)}{\text{tr}(\hat{\Sigma}_G) + \text{tr}(\hat{\Sigma}_E)}$ (58). Note that $\text{tr}(\hat{\Sigma}_G) = \frac{1}{v_k} \text{tr}[(K - \tau I) Y Y^\top] = \frac{1}{\kappa - \tau^2} \text{tr}[(K - \tau I) \hat{\Sigma}_P]$, where $\hat{\Sigma}_P = Y Y^\top / N$ is the estimated phenotypic covariance matrix. Similarly, $\text{tr}(\hat{\Sigma}_E) = \frac{1}{\kappa - \tau^2} \text{tr}[(\kappa I - \tau K) \hat{\Sigma}_P]$. For any nonnegative definite phenotypic similarity matrix $\hat{\Lambda}_P$ derived from a nonlinear measure, we define heritability by replacing $\hat{\Sigma}_P$ with $\hat{\Lambda}_P$. This is known as the kernel trick in machine learning. We note that for any $N \times N$ nonnegative definite matrix Σ, there exists a $N \times P$ matrix V (often $P \ll N$) such that $\Sigma \approx V V^\top$. Therefore, Σ can be considered as a linear covariance matrix generated by a multidimensional trait.

To model covariates, consider a multivariate mixed effects model: $Y = XB + G + E$, where X is an $N \times q$ matrix of covariates, and B is a $q \times M$ matrix of fixed effects. There exists an $N \times (N - q)$ matrix U satisfying $U^\top U = I$, $U U^\top = P_0 = I - X(X^\top X)^{-1} X$, and $U^\top X = 0$. Applying $U^\top$ to both sides of the model gives $U^\top Y = U^\top G + U^\top E$, where $\text{vec}(U^\top G) \sim N(0, \Sigma_G \otimes (U^\top K U))$, $\text{vec}(U^\top E) \sim N(0, \Sigma_E \otimes I)$. Therefore, we can replace Y with $U^\top Y$, K with $U^\top K U$, and N with $N - q$ in the SNP heritability estimator derived above to obtain an estimator that accounts for covariates. More specifically, $\text{tr}(\hat{\Sigma}_G) = \frac{1}{\kappa - \tau^2} \text{tr}[(K - \tau I) P_0 \hat{\Sigma}_P P_0]$, $\text{tr}(\hat{\Sigma}_E) = \frac{1}{\kappa - \tau^2} \text{tr}[(\kappa I - \tau K) P_0 \hat{\Sigma}_P P_0]$, $\tau = \text{tr}(K P_0)/(N - q)$, and $\kappa = \text{tr}(K P_0 K P_0)/(N - q)$. For nonlinear phenotypic similarity matrix $\hat{\Lambda}_P$, we replace $\hat{\Sigma}_P$ with $\hat{\Lambda}_P$.

Significance was measured using subject-based permutations in which the kinship matrix was randomly shuffled 1,000 times. SEs were calculated using a block jackknife procedure with a leave one family out strategy. That is, for a given iteration of the jackknife, all participants within a nuclear family unit were excluded and heritability was recalculated. Variability was then calculated from the resulting distribution of subsampled heritability estimates.

Data Availability. All custom code written to perform analyses are publicly available on GitHub (https://github.com/kevmanderson/heritable_network_topography). We have also provided an open-access generalized implementation of our multidimensional heritability estimator (https://github.com/kevmanderson/h2_multi). Code to produce individualized MS-HBM parcellations is publicly available (https://github.com/ThomasYeoLab/CBIG). The HCP data used in this study are available through the database at https://db.humanconnectome.org/.

Table 1. HCP group demographics

	MZ	DZ	Nontwin	Singleton	F	P
n	274	160	482	107		
Age	29.0 (SD = 3.36)	29.4 (SD = 3.61)	28.4 (SD = 3.86)	28.3 (SD = 3.71)	$F_{3,1019} = 4.62$	0.003
Sex	F = 59.9%	F = 61.2%	F = 49.6%	F = 48.6%	$F_{3,1019} = 4.10$	0.006

Heritability estimates were conducted on 1,023 HCP participants, composed of 137 MZ twins ($n = 274$), 80 DZ twins ($n = 160$), nontwin siblings ($n = 482$), and unrelated singletons ($n = 107$). Although groups were nominally well matched demographically, ANOVAs revealed significant differences of age and sex. All heritability analyses included age and sex as covariates.

Anderson et al.
Heritability of individualized cortical network topography

PNAS | 7 of 9
https://doi.org/10.1073/pnas.2016271118

www.manaraa.com

1. P. S. Goldman-Rakic, Topography of cognition: Parallel distributed networks in primate association cortex. *Annu. Rev. Neurosci.* **11**, 137–156 (1988).
2. B. Biswal, F. Z. Yetkin, V. M. Haughton, J. S. Hyde, Functional connectivity in the motor cortex of resting human brain using echo-planar MRI. *Magn. Reson. Med.* **34**, 537–541 (1995).
3. C. F. Beckmann, M. DeLuca, J. T. Devlin, S. M. Smith, Investigations into resting-state connectivity using independent component analysis. *Philos. Trans. R. Soc. Lond. B Biol. Sci.* **360**, 1001–1013 (2005).
4. J. S. Damoiseaux *et al.*, Consistent resting-state networks across healthy subjects. *Proc. Natl. Acad. Sci. U.S.A.* **103**, 13848–13853 (2006).
5. N. U. F. Dosenbach *et al.*, Distinct brain networks for adaptive and stable task control in humans. *Proc. Natl. Acad. Sci. U.S.A.* **104**, 11073–11078 (2007).
6. M. D. Fox, M. Corbetta, A. Z. Snyder, J. L. Vincent, M. E. Raichle, Spontaneous neuronal activity distinguishes human dorsal and ventral attention systems. *Proc. Natl. Acad. Sci. U.S.A.* **103**, 10046–10051 (2006).
7. J. D. Power *et al.*, Functional network organization of the human brain. *Neuron* **72**, 665–678 (2011).
8. B. T. T. Yeo *et al.*, The organization of the human cerebral cortex estimated by intrinsic functional connectivity. *J. Neurophysiol.* **106**, 1125–1165 (2011).
9. R. M. Braga, R. L. Buckner, Parallel interdigitated distributed networks within the individual estimated by intrinsic functional connectivity. *Neuron* **95**, 457–471.e5 (2017).
10. M. Chong *et al.*, Individual parcellation of resting fMRI with a group functional connectivity prior. *Neuroimage* **156**, 87–100 (2017).
11. E. M. Gordon *et al.*, Individual-specific features of brain systems identified with resting state functional correlations. *Neuroimage* **146**, 918–939 (2017).
12. E. M. Gordon *et al.*, Precision functional mapping of individual human brains. *Neuron* **95**, 791–807.e7 (2017).
13. R. Kong *et al.*, Spatial topography of individual-specific cortical networks predicts human cognition, personality, and emotion. *Cereb. Cortex* **29**, 2533–2551 (2019).
14. T. O. Laumann *et al.*, Functional system and areal organization of a highly sampled individual human brain. *Neuron* **87**, 657–670 (2015).
15. D. Wang *et al.*, Parcelling cortical functional networks in individuals. *Nat. Neurosci.* **18**, 1853–1860 (2015).
16. C. Gratton *et al.*, Defining individual-specific functional neuroanatomy for precision psychiatry. *Biol. Psychiatry* **88**, 28–39 (2020).
17. L. Mwilambwe-Tshilobo *et al.*, Loneliness and meaning in life are reflected in the intrinsic network architecture of the brain. *Soc. Cogn. Affect. Neurosci.* **14**, 423–433 (2019).
18. R. A. Ozdemir *et al.*, Individualized perturbation of the human connectome reveals reproducible biomarkers of network dynamics relevant to cognition. *Proc. Natl. Acad. Sci. U.S.A.* **117**, 8115–8125 (2020).
19. P. K. Reardon *et al.*, Normative brain size variation and brain shape diversity in humans. *Science* **360**, 1222–1227 (2018).
20. T. Kaufmann *et al.*, Delayed stabilization and individualization in connectome development are related to psychiatric disorders. *Nat. Neurosci.* **20**, 513–515 (2017).
21. M. W. Cole, D. S. Bassett, J. D. Power, T. S. Braver, S. E. Petersen, Intrinsic and task-evoked network architectures of the human brain. *Neuron* **83**, 238–251 (2014).
22. N. A. Crossley *et al.*, Cognitive relevance of the community structure of the human brain functional coactivation network. *Proc. Natl. Acad. Sci. U.S.A.* **110**, 11583–11588 (2013).
23. F. M. Krienen, B. T. T. Yeo, R. L. Buckner, Reconfigurable task-dependent functional coupling modes cluster around a core functional architecture. *Philos. Trans. R. Soc. Lond. B Biol. Sci.* **369**, 20130526 (2014).
24. T. He *et al.*, Deep neural networks and kernel regression achieve comparable accuracies for functional connectivity prediction of behavior and demographics. *Neuroimage* **206**, 116276 (2020).
25. M. D. Rosenberg *et al.*, A neuromarker of sustained attention from whole-brain functional connectivity. *Nat. Neurosci.* **19**, 165–171 (2016).
26. S. M. Smith *et al.*, A positive-negative mode of population covariation links brain connectivity, demographics and behavior. *Nat. Neurosci.* **18**, 1565–1567 (2015).
27. J. T. Baker *et al.*, Functional connectomics of affective and psychotic pathology. *Proc. Natl. Acad. Sci. U.S.A.* **116**, 9050–9059 (2019).
28. T. Ge, A. J. Holmes, R. L. Buckner, J. W. Smoller, M. R. Sabuncu, Heritability analysis with repeat measurements and its application to resting-state functional connectivity. *Proc. Natl. Acad. Sci. U.S.A.* **114**, 5521–5526 (2017).
29. D. C. Glahn *et al.*, Genetic control over the resting brain. *Proc. Natl. Acad. Sci. U.S.A.* **107**, 1223–1228 (2010).
30. O. Miranda-Dominguez *et al.*, Heritability of the human connectome: A connectotyping study. *Netw. Neurosci.* **2**, 175–199 (2018).
31. B. Zhao *et al.*, Common variants contribute to intrinsic human brain functional networks. *bioRxiv* [Preprint] (2020). https://doi.org/10.1101/2020.07.30.229914 (Accessed 21 October 2020).
32. E. S. Finn *et al.*, Functional connectome fingerprinting: Identifying individuals using patterns of brain connectivity. *Nat. Neurosci.* **18**, 1664–1671 (2015).
33. J. M. Reinen *et al.*, The human cortex possesses a reconfigurable dynamic network architecture that is disrupted in psychosis. *Nat. Commun.* **9**, 1157 (2018).
34. K. M. Anderson *et al.*, Gene expression links functional networks across cortex and striatum. *Nat. Commun.* **9**, 1428 (2018).
35. F. M. Krienen, B. T. T. Yeo, T. Ge, R. L. Buckner, C. C. Sherwood, Transcriptional profiles of supragranular-enriched genes associate with corticocortical network architecture in the human brain. *Proc. Natl. Acad. Sci. U.S.A.* **113**, E469–E478 (2016).
36. J. Richiardi *et al.*; IMAGEN consortium, BRAIN NETWORKS. Correlated gene expression supports synchronous activity in brain networks. *Science* **348**, 1241–1244 (2015).
37. L. Han *et al.*, Functional parcellation of the cerebral cortex across the human adult lifespan. *Cereb. Cortex* **28**, 4403–4423 (2018).
38. M. Salehi, A. Karbasi, X. Shen, D. Scheinost, R. T. Constable, An exemplar-based approach to individualized parcellation reveals the need for sex specific functional networks. *Neuroimage* **170**, 54–67 (2018).
39. J. D. Power, B. L. Schlaggar, C. N. Lessov-Schlaggar, S. E. Petersen, Evidence for hubs in human functional brain networks. *Neuron* **79**, 798–813 (2013).
40. B. A. Seitzman *et al.*, Trait-like variants in human functional brain networks. *Proc. Natl. Acad. Sci. U.S.A.* **116**, 22851–22861 (2019).
41. J. D. Bijsterbosch *et al.*, The relationship between spatial configuration and functional connectivity of brain regions. *eLife* **7**, e32992 (2018).
42. Z. Cui *et al.*, Individual variation in functional topography of association networks in youth. *Neuron* **106**, 340–353.e8 (2020).
43. S. Mueller *et al.*, Individual variability in functional connectivity architecture of the human brain. *Neuron* **77**, 586–595 (2013).
44. G. L. Colclough *et al.*, The heritability of multi-modal connectivity in human brain activity. *eLife* **6**, e20178 (2017).
45. Z. Yang *et al.*, Genetic and environmental contributions to functional connectivity architecture of the human brain. *Cereb. Cortex* **26**, 2341–2352 (2016).
46. D. C. Van Essen *et al.*; Wu-Minn HCP Consortium, Data from "Human connectome project." ConnectomeDB. https://db.humanconnectome.org/. Accessed 1 January 2019.
47. J. Sepulcre *et al.*, The organization of local and distant functional connectivity in the human brain. *PLoS Comput. Biol.* **6**, e1000808 (2010).
48. D. C. Van Essen, D. L. Dierker, Surface-based and probabilistic atlases of primate cerebral cortex. *Neuron* **56**, 209–225 (2007).
49. L. Almasy, J. Blangero, Multipoint quantitative-trait linkage analysis in general pedigrees. *Am. J. Hum. Genet.* **62**, 1198–1211 (1998).
50. R. L. Buckner, F. M. Krienen, The evolution of distributed association networks in the human brain. *Trends Cogn. Sci.* **17**, 648–665 (2013).
51. D. C. Van Essen, A tension-based theory of morphogenesis and compact wiring in the central nervous system. *Nature* **385**, 313–318 (1997).
52. K. M. Anderson *et al.*, Transcriptional and imaging-genetic association of cortical interneurons, brain function, and schizophrenia risk. *Nat. Commun.* **11**, 2889 (2020).
53. D. D. M. O'Leary, S.-J. Chou, S. Sahara, Area patterning of the mammalian cortex. *Neuron* **56**, 252–269 (2007).
54. C. R. Cadwell, A. Bhaduri, M. A. Mostajo-Radji, M. G. Keefe, T. J. Nowakowski, Development and arealization of the cerebral cortex. *Neuron* **103**, 980–1004 (2019).
55. D. Boomsma, A. Busjahn, L. Peltonen, Classical twin studies and beyond. *Nat. Rev. Genet.* **3**, 872–882 (2002).
56. C.-H. Chen *et al.*, Hierarchical genetic organization of human cortical surface area. *Science* **335**, 1634–1636 (2012).
57. T. Ge *et al.*, Massively expedited genome-wide heritability analysis (MEGHA). *Proc. Natl. Acad. Sci. U.S.A.* **112**, 2479–2484 (2015).
58. M. S. Panizzon *et al.*, Distinct genetic influences on cortical surface area and cortical thickness. *Cereb. Cortex* **19**, 2728–2735 (2009).
59. T. Ge *et al.*, Multidimensional heritability analysis of neuroanatomical shape. *Nat. Commun.* **7**, 13291 (2016).
60. J. Seidlitz *et al.*; NSPN Consortium, Morphometric similarity networks detect microscale cortical organization and predict inter- individual cognitive variation. *Neuron* **97**, 231–247.e7 (2018).
61. M. R. Sabuncu *et al.*; Alzheimer's Disease Neuroimaging Initiative, Morphometricity as a measure of the neuroanatomical signature of a trait. *Proc. Natl. Acad. Sci. U.S.A.* **113**, E5749–E5756 (2016).
62. T. J. C. Polderman *et al.*, Meta-analysis of the heritability of human traits based on fifty years of twin studies. *Nat. Genet.* **47**, 702–709 (2015).
63. D. H. Geschwind, P. Rakic, Cortical evolution: Judge the brain by its cover. *Neuron* **80**, 633–647 (2013).
64. P. Rakic, Specification of cerebral cortical areas. *Science* **241**, 170–176 (1988).
65. K. L. Grasby *et al.*; Alzheimer's Disease Neuroimaging Initiative; CHARGE Consortium; EPIGEN Consortium; IMAGEN Consortium; SYS Consortium; Parkinson's Progression Markers Initiative; Enhancing NeuroImaging Genetics through Meta-Analysis Consortium (ENIGMA)—Genetics working group, The genetic architecture of the human cerebral cortex. *Science* **367**, 1–14 (2020).

Anderson et al.
Heritability of individualized cortical network topography

www.manaraa.com

66. C. Llinares-Benadero, V. Borrell, Deconstructing cortical folding: Genetic, cellular and mechanical determinants. *Nat. Rev. Neurosci.* **20**, 161–176 (2019).

67. C. Dehay, G. Horsburgh, M. Berland, H. Killackey, H. Kennedy, Maturation and connectivity of the visual cortex in monkey is altered by prenatal removal of retinal input. *Nature* **337**, 265–267 (1989).

68. V. Moreno-Juan *et al.*, Prenatal thalamic waves regulate cortical area size prior to sensory processing. *Nat. Commun.* **8**, 14172 (2017).

69. T. Reed, R. J. Viken, S. A. Rinehart, High heritability of fingertip arch patterns in twin-pairs. *Am. J. Med. Genet. A.* **140**, 263–271 (2006).

70. A. Fornito *et al.*, Genetic influences on cost-efficient organization of human cortical functional networks. *J. Neurosci.* **31**, 3261–3270 (2011).

71. Y. Fu *et al.*, Genetic influences on resting-state functional networks: A twin study. *Hum. Brain Mapp.* **36**, 3959–3972 (2015).

72. B. Sinclair *et al.*, Heritability of the network architecture of intrinsic brain functional connectivity. *Neuroimage* **121**, 243–252 (2015).

73. J. E. Schmitt *et al.*, The dynamic role of genetics on cortical patterning during childhood and adolescence. *Proc. Natl. Acad. Sci. U.S.A.* **111**, 6774–6779 (2014).

74. S. E. Bergen, C. O. Gardner, K. S. Kendler, Age-related changes in heritability of behavioral phenotypes over adolescence and young adulthood: A meta-analysis. *Twin Res. Hum. Genet.* **10**, 423–433 (2007).

75. T. Ge, C.-Y. Chen, B. M. Neale, M. R. Sabuncu, J. W. Smoller, Phenome-wide heritability analysis of the UK Biobank. *PLoS Genet.* **13**, e1006711 (2017).

76. D. G. Gee *et al.*, Early developmental emergence of human amygdala-prefrontal connectivity after maternal deprivation. *Proc. Natl. Acad. Sci. U.S.A.* **110**, 15638–15643 (2013).

77. M. J. Arcaro, P. F. Schade, J. L. Vincent, C. R. Ponce, M. S. Livingstone, Seeing faces is necessary for face-domain formation. *Nat. Neurosci.* **20**, 1404–1412 (2017).

78. B. J. Casey *et al.*; ABCD Imaging Acquisition Workgroup, The adolescent brain cognitive development (ABCD) study: Imaging acquisition across 21 sites. *Dev. Cogn. Neurosci.* **32**, 43–54 (2018).

79. L. T. Elliott *et al.*, Genome-wide association studies of brain imaging phenotypes in UK Biobank. *Nature* **562**, 210–216 (2018).

80. M. F. Glasser *et al.*, The human connectome project's neuroimaging approach. *Nat. Neurosci.* **19**, 1175–1187 (2016).

81. M. F. Glasser *et al.*, A multi-modal parcellation of human cerebral cortex. *Nature* **536**, 171–178 (2016).

82. S. M. Smith *et al.*; WU-Minn HCP Consortium, Resting-state fMRI in the human connectome project. *Neuroimage* **80**, 144–168 (2013).

83. D. C. Van Essen *et al.*; WU-Minn HCP Consortium, The WU-Minn human connectome project: An overview. *Neuroimage* **80**, 62–79 (2013).

84. M. F. Glasser *et al.*; WU-Minn HCP Consortium, The minimal preprocessing pipelines for the human connectome project. *Neuroimage* **80**, 105–124 (2013).

85. D. S. Marcus *et al.*, Informatics and data mining tools and strategies for the human connectome project. *Front. Neuroinform.* **5**, 4 (2011).

Anderson et al.
Heritability of individualized cortical network topography

www.manaraa.com